Chemical Engineering Journal 94 (2003) 179–187

Chemical Engineering Journal

www.elsevier.com/locate/cej

Pressure drop for two phase counter-current flow in a packed column with a novel internal

Minghan Han*, Hongfei Lin, Yanhui Yuan, Dezheng Wang, Yong Jin

Department of Chemical Engineering, Tsinghua University, Beijing 100084, PR China

Received 29 May 2002; accepted 8 February 2003

Abstract

A novel internal made of several structured porous passages can eliminate excessive pressure drop and "flooding" in a packed column with conventional gas liquid counter-current flow. A pressure drop model is developed on the assumption that the internal part divides the gas flow into two branches, one of which contacts the liquid in a conventional counter-current flow and the other in a new cross current flow. The model shows that the gas velocity for counter-current flow in a column with these internal parts of 15–30% volume fraction is about 5–30% of that without the internal parts and more gas flows in the cross current pattern. Decreases in the gas velocity and liquid hold-up make the pressure drop low.
© 2003 Elsevier Science B.V. All rights reserved.

Keywords: Catalytic distillation; Internal; Pressure drop; Cross flow; Counter-current flow; Model

1. Introduction

Reactive distillation (RD), which combines reaction and distillation, has been a focus of research in the chemical process industry and academia in the last decade [1–3]. The benefits of RD can be summarized as follows [4]: simplification or elimination of the separation system, improved conversion that can approach 100%, improved selectivity, significantly reduced quantity of catalyst for the same degree of conversion, avoidance of azeotropes, reduced by-product formation, heat integration benefits and avoidance of hot spot and runaways using liquid vaporization as a thermal fly wheel.

A RD application requires the consideration of some practical issues [5], such as, efficient contacting of liquid with catalyst particles, good vapor–liquid contacting in the reactive zone, low pressure drop through the catalytically packed reactive section, sufficient liquid hold-up in the reactive section, and easy installation and removal of the RD equipment and catalyst. Numerous patents and research reports give catalyst loading methods designed to meet the above practical requirements. Some of the most popular catalysts loading methods are as follows: (1) catalyst baskets on trays, (2) catalytic random packings, (3) catalyst-containing bales or structured catalyst supports like Katapak®-S.

Although some of these catalysts loading methods above have been used in industry, there have yet been no devices that allow on-line removal and regeneration of catalyst. If the catalyst deactivates, regeneration has to be done ex situ and so there must be provisions for the easy removal and installation of catalyst particles. RD is often passed over as a processing option because catalyst deactivation would require frequent shutdowns.

In the conventional catalysts loading methods, the catalyst particles in a RD column are enveloped and divided into many parts by baskets, bales, or wire gauze etc, that is, the catalyst is in "dispersed phases". To allow an on-stream removal of the catalyst, the catalyst must be outside the envelopes and contained in a "continuous phase".

A novel RD device [6] that allows on-stream removal of catalyst solves the above problem. In this device, a novel internal part is installed inside the column, and the catalyst particles are loaded in the same way as they are loaded into a fixed bed reactor. Thus on-stream installation and removal of the catalyst are easily realized. The cold model and hot model experiments [7,8] showed that a RD column with the novel internal part has many advantages such as low pressure, simple structure, low operating cost, convenience of installation and removal of catalyst, and a large catalyst loading fraction.

The pressure drop is one of the most important parameters in the design of a RD bed, even for predicting gas–liquid and liquid–solid mass transfer [9]. Numerous attempts [10–16]

* Corresponding author. Tel.: +86-10-62781469; fax: +86-10-62772051.
E-mail address: hanmh@flotu.org (M. Han).

1385-8947/03/$ – see front matter © 2003 Elsevier Science B.V. All rights reserved.
doi:10.1016/S1385-8947(03)00059-7

Nomenclature

a	geometrical area of packing (m^2/m^3)
a, b, c, d, e	parameters
d_P	diameter of the particles (m)
d'_P	diameter of the irrigated particles (m)
F	volume fraction of the internal (dimensionless)
h	liquid hold-up in catalyst bed (m^3/m^3)
H	height of the column (m)
K_1 and K_2	coefficients (dimensionless)
K_M and K'_M	friction factors (dimensionless)
l_b	height of the stage between two baffles (m)
n	number of the stages in a spring divided by the baffles
N	number of springs in the column
ΔP, $\Delta P'$	pressure drop of per unit bed height (Pa/m)
ΔP_B	friction loss for the gas radial flow through catalytic bed (Pa)
ΔP_F	wall friction of the gas flow though the springs (Pa)
ΔP_I	friction loss for the gas radial flow through the interface (Pa)
ΔP_M	momentum lose arising from the change of gas flow direction (Pa)
ΔP_S	sum of pressure drops per stage of the springs (Pa)
r	radius of the springs (m)
$\Delta\bar{r}$	equivalent radial distance (m)
R	inside radius of the column (m)
Re	Reynolds number (dimensionless)
u_B	effective axial gas velocity in catalyst bed (m/s)
$u_{B,0}$	superficial axial gas velocity in catalyst bed (m/s)
u_G	superficial gas velocity in column (m/s)
u_L	effective axial liquid velocity in catalyst bed (m/s)
$u_{L,0}$	superficial axial liquid velocity in column (m/s)
u_P	effective axial gas velocity in porous passages (springs) (m/s)
$u_{P,0}$	superficial axial gas velocity in porous passages (springs) (m/s)
Z	height in vertical direction (m)

Greek letters

ε	void fraction in dry bed (dimensionless)
ε'	void fraction in irrigated bed (dimensionless)
ϕ	gas friction factor (dimensionless)
μ	viscosity (N s/m^2)
ρ	density of gas (kg/m^3)
ω_0	superficial radial gas flow velocity in the catalyst bed (m/s)
ω	effective radial gas flow velocity in the catalyst bed (m/s)

Subscripts

G	gas
L	liquid

have been made to describe the hydrodynamic behavior of packed columns operating as countercurrent gas–liquid contactors. The basic approaches to describing the hydrodynamics of a packed column are the channel model and the particle model. In the first, the gas is assumed to flow upwards inside numerous small channels having the same characteristic dimension; as liquid flows down the 'walls' of the same channels it reduces the available cross-sectional area for gas flow, thus causing increased pressure drop. In the particle model the gas is assumed to flow around a packing particle of a characteristic dimension and the liquid acts to increase this dimension by its adherence to the particle surface. The presence of the liquid also reduces the void fraction of the bed. These attempts have ranged from the very empirical to semi-empirical and have achieved moderate success for some applications within certain limited ranges of operating conditions.

However, the pressure drop in the column with the new internal is about 1/10 as that in the column without the internal, and it depends on not only the properties and flow behavior of fluid, but also the geometric parameters of the internal [7,8]. Obviously, the internal changes the flow behavior of fluid and a new flow behavior is formed, so the traditional models [10–17] cannot be used to calculate the pressure drop in the column with the internal which is determined by several geometric parameters. To calculate the pressure drop, the pressure model must be correlated with the new flow behavior of fluid and the geometric parameters.

In this present work, a particle model has been developed to compute pressure drop not only for a better understanding of the mechanism of the novel internal part but also for developing necessary information for design and scale-up purposes.

2. Experiments

A schematic drawing of the cold model experimental apparatus is shown in Fig. 1. The column is a Plexiglas tube of 140 mm i.d. Air and water at normal temperature and pressure are used as test fluids. For the solid phase, porcelain balls with an average diameter of about 5 mm are used and the bulk void fraction is 0.4. The flow rates of liquid and gas are determined by rotameters. The pressure drop is measured by a differential pressure meter.

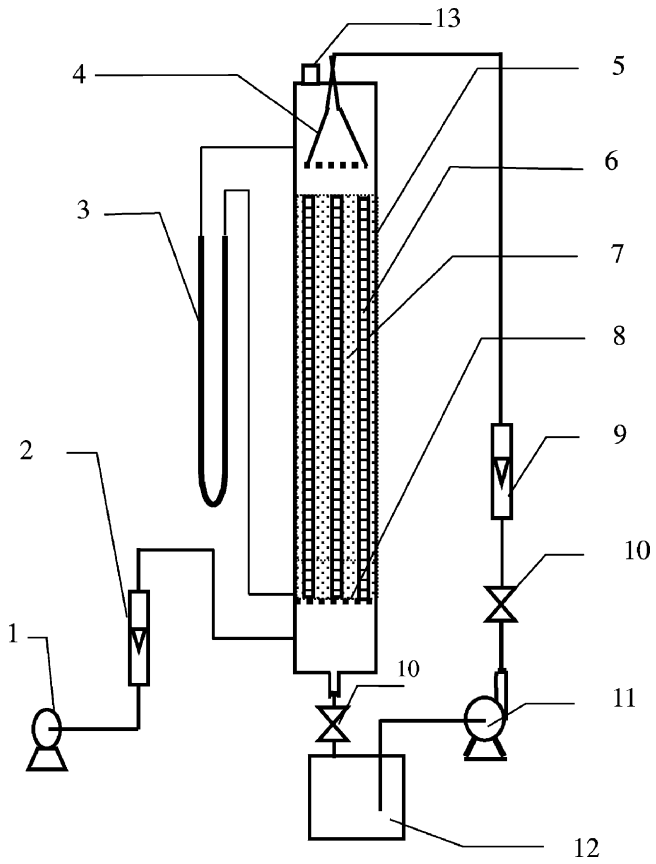

Fig. 1. Schematic drawing of the cold model experimental apparatus for a counter-current flow in a packed column with a novel internal. 1: Air blower; 2: gas rotameter; 3: differential pressure meter; 4: liquid distributor; 5: column; 6: internal; 7: porcelain balls; 8: gas distributor; 9: liquid rotameters; 10: valve; 11: pump; 12: water tank; 13: gas vent.

The cold model experiment is conducted as follows: gas from the blower enters the bottom of the RD column through the gas distributor, then flows upward through the catalyst bed and finally vents out from the air exit at the top of the column. Similarly, water from the water tank enters the top of the column through the liquid distributor, flows downward through the catalyst bed (i.e. the ball bed in the cold experiments) and exits from the drain outlet at the bottom of the column to the water tank.

A schematic drawing of the structure of the novel internal parts and the catalyst loading method is shown in Fig. 2. The internal parts function as porous passages that form gas and liquid flow channels. These passages are mounted in a frame and placed into the column vertically. The catalyst particles are dumped into the column and fill the space between the passages and thus on-stream installation and removal of catalyst are easily realized. Openings are provided in the retaining screens of the passages to allow gas and liquid to flow into or out of the passage. These openings are sized to prevent the catalyst particles from entering the passages. Each passage is separated into several stages by baffles. The baffles are installed alternately between adjacent passages.

In this work spiral springs are used as the retaining screen of the passages. The opening ratio on the wall of the spiral spring (retaining screens of the passages) is 50%, and the height of the internals is 1 m. The heights of the stages between the baffles for each internal are 62.5, 125, and 250 mm, respectively. The other geometric parameters of the different spiral spring internals are shown in Table 1.

Table 1
Main geometric parameters of the different spiral spring internals

Serial number of internals	Numbers of spiral springs	Outer diameter of the springs (m)	Volume fraction of the internal in the column (F)	Height of the stage between two baffles, l_b (m)
1	5	0.025	0.159	0.0625
2	–	–	–	0.125
3	–	–	–	0.250
4	7	0.025	0.223	0.0625
5	–	–	–	0.125
6	–	–	–	0.250
7	9	0.025	0.287	0.0625
8	–	–	–	0.125
9	–	–	–	0.250
10	5	0.035	0.313	0.0625
11	–	–	–	0.125
12	–	–	–	0.250
13	3	0.045	0.310	0.0625
14	–	–	–	0.125
15	–	–	–	0.250

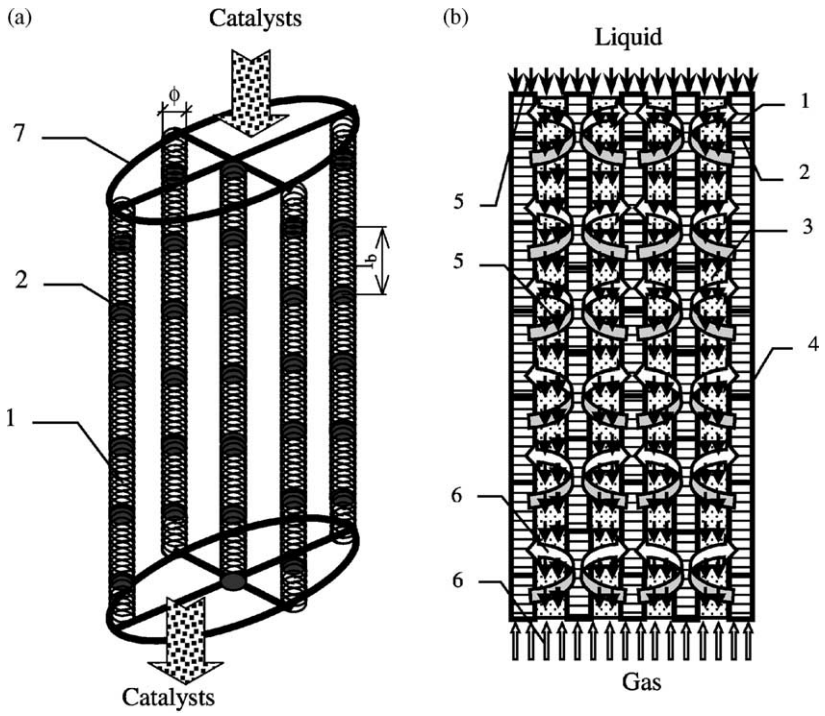

Fig. 2. (a and b) Schematic of the novel internal and catalyst loading method. 1: Spiral spring (retaining screen of passage); 2: baffle; 3: catalyst pellets; 4: column wall; 5: liquid flow; 6: gas flow; 7: frame.

3. Pressure drop model

To establish a pressure drop model, an ideal flow pattern [18] of gas and liquid in the column is assumed as shown in Fig. 3. The internal part divides the gas flow into two branches: one contacts the liquid in a conventional counter-current flow and the other does so in a new cross current flow, that is, the gas and liquid flows in the catalyst bed consists of a conventional counter-current pattern and a new cross current pattern.

In the conventional flow pattern, gas flows upwards and liquid flows downwards, and they contact in a counter-current pattern in the catalyst bed.

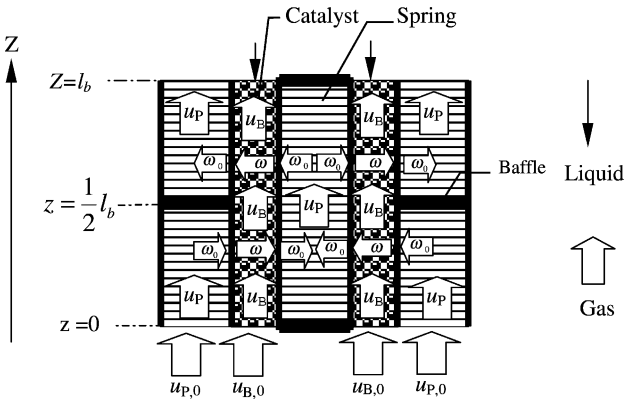

Fig. 3. Ideal flow patterns of gas and liquid in the column.

In the new flow pattern, shown in Figs. 2(b) and Fig. 3, gas and liquid flow behaviors are different from those of the conventional flow pattern. For the gas flow, gas flows upwards (axially) inside the springs, changes the flow direction, and subdivides uniformly through the wall of the springs into the catalyst bed when it is blocked by the baffles, then, flows radially through the catalyst bed into adjacent springs; thus, the gas contacts the liquid in a cross current pattern in the catalyst bed. After entering the adjacent springs from the catalyst bed, the gas will change its flow direction and flows upwards again. Gas enters the stage from the lower half portion and leaves the stage from the upper half portion continuously. For the liquid flow, when the liquid load is below the load point, the space between the catalyst particles is not totally filled with liquid and capillary effects draw the liquid into the catalyst bed; when the liquid load is above the load point, the excess liquid leaves the catalyst bed and goes into the internal, namely liquid fills in both the catalyst bed and internal.

Upon entering the column, the gas is divided into two branches. One enters the porous passages (springs), and the other enters the catalyst bed.

$$\pi R^2 F u_{P,0} + \pi R^2 (1 - F) u_{B,0} = \pi R^2 u_G \quad (1)$$

that is,

$$F u_{P,0} + (1 - F) u_{B,0} = u_G \quad (2)$$

where $u_{P,0}$ and $u_{B,0}$ are the superficial axial gas velocities in the porous passages (springs) and the catalyst bed,

respectively, u_G the superficial gas velocities in the column, R the inside radius of the column, and F is volume fraction of the internal.

For the counter-current flow, the pressure drop ΔP per unit bed height can be calculated by the Ergun equation as follows:

$$\Delta P = 150\frac{\mu_G(1-\varepsilon)^2 u_{B,0}}{d_P^2\varepsilon^3} + 1.75\frac{\rho_G(1-\varepsilon)u_{B,0}^2}{d_P\varepsilon^3} \quad (3)$$

or

$$\Delta P = \left(\frac{4.17}{Re_G} + 0.29\right)\frac{(1-\varepsilon)a}{\varepsilon^3}\rho_G u_{B,0}^2 \quad (3')$$

where ε is void fraction of catalyst bed and d_P is diameter of particles.

For the cross current flow, the pressure drop per stage of the springs, ΔP_S, is given by the sum of wall friction due to the axial gas flow though the springs, ΔP_F, momentum loss arising from the change of gas flow direction, ΔP_M, friction loss for the gas radial flow through the interface between the wall of the springs and catalytic bed, ΔP_I and that through catalytic bed, ΔP_B. It can be expressed by Eq. (4).

$$\Delta P_S = \Delta P_F + \Delta P_M + \Delta P_I + \Delta P_B \quad (4)$$

For gas flow in the upper half portion of the springs stage (Fig. 3), $0.5l_b \le z \le l_b$,

$$\pi r^2 u_P = \pi r^2 u_{P,0} - 2\pi r\left(z - \frac{1}{2}l_b\right)\omega_0 \quad (5)$$

where l_b is height of the stage between two baffles, u_P the effective axial gas flow velocity in the springs, r the radius of the springs, and ω_0 is superficial radial gas flow velocity which can be calculated as follows:

$$\omega_0 = \frac{\pi r^2 u_{P,0}}{2\pi r(l_b/2)} = \frac{r u_{P,0}}{l_b} \quad (6)$$

Combining Eqs. (5) and (6),

$$u_P = \left(2 - \frac{2z}{l_b}\right)u_{P,0} \quad (7)$$

For gas flow in the lower half portion of the stage, $0 \le z \le 0.5l_b$,

$$\pi r^2 u_P = 2\pi r z\omega_0 \quad (8)$$

Combining Eqs. (6) and (8),

$$u_P = \frac{2z}{l_b}u_{P,0} \quad (9)$$

The detailed expressions for each term of Eq. (4) in the dry case as well the irrigated case are discussed in the following sections.

3.1. Dry pressure drop

3.1.1. Wall friction of the gas flow though the springs, ΔP_F

When the gas flow rate along the stages is changed continuously without liquid flowing in the column, friction loss by the gas flow though the springs ΔP_F in one stage can be expressed as follows:

$$\Delta P_F = \int_0^{l_b} \frac{2\phi\rho_G u_P^2}{r}\,dZ \quad (10)$$

where ϕ is gas friction factor, which can be between 0.004 and 0.01 [19]. Substituting Eqs. (7) and (9) into Eq. (10) and simplifying:

$$\Delta P_F = \frac{2\phi\rho_G l_b u_{P,0}^2}{3r} \quad (11)$$

3.1.2. Momentum loss due to the change of gas flow direction, ΔP_M

For two adjacent springs, the flow direction changes four times. The resistance loss from the flow direction changes ΔP_M is expressed by [20,21]:

$$\Delta P_M = 2\left(K_M\rho_G\frac{\omega_0^2}{2} + K'_M\rho_G\frac{u_{P,0}^2}{2}\right) \quad (12)$$

where friction factors, K_M and K'_M, can be taken to be between 0.6 and 1.2 [19] since the gas makes a 90° change in direction.

3.1.3. Friction loss for gas radial flow through the interface, ΔP_I

ΔP_I can be regarded as the friction loss from the sudden enlargement and sudden contraction of gas flow in the pipes. It can be expressed as follows [19]:

$$\Delta P_I = 2\left(K_1\frac{\rho_G(\omega^2 - \omega_0^2)}{2} + K_2\frac{\rho_G\omega^2}{2}\right) \quad (13)$$

where the first term of Eq. (13) is the friction loss from the sudden enlargement, the second term is that of the sudden contraction. K_1 and K_2 are coefficients, which are less than 1 and 0.67, respectively [19]. ω is the effective radial gas flow velocity in the catalytic bed,

$$\omega = \frac{\omega_0}{\varepsilon} \quad (14)$$

3.1.4. Friction loss for radial flow of the gas through the catalyst bed, ΔP_B

The pressure drop ΔP_B can be calculated by the Ergun equation:

$$\Delta P_B = 2\left[150\frac{\mu(1-\varepsilon)^2\omega_0}{d_P^2\varepsilon^3} + 1.75\frac{\rho_G(1-\varepsilon)\omega_0^2}{d_P\varepsilon^3}\right]\Delta\bar{r} \quad (15)$$

or

$$\Delta P_B = 2\left[\left(\frac{4.17}{Re_G} + 0.29\right)\frac{(1-\varepsilon)a}{\varepsilon^3}\rho\varpi_0^2\right]\Delta\bar{r} \quad (15')$$

where $\Delta\bar{r}$, an equivalent radial distance, is the distance of gas flow between two adjacent springs. It can be written as:

$$\frac{\pi R^2 H - N\pi r^2 H}{N} = \pi(\Delta\bar{r} + r)^2 H - \pi r^2 H \quad (16)$$

so

$$\Delta\bar{r} = \sqrt{\frac{1}{N}}(R - r) \tag{17}$$

3.1.5. Pressure drop per unit bed height, $\Delta P'$

Substituting Eqs. (11)–(13) and (15) into Eq. (4) and simplifying, the total pressure drop per unit bed height is:

$$\begin{aligned}\Delta P' &= \frac{\Delta P_S}{l_b} \\ &= \frac{1}{l_b}\left\{\frac{2\phi\rho_G l_b u_{P,0}^2}{3r} + 2K_M\rho_G\frac{\omega_0^2}{2} + 2K'_M\rho_G\frac{u_{P,0}^2}{2}\right. \\ &\quad + 2K_1\frac{\rho_G(\omega^2-\omega_0^2)}{2} + 2K_2\frac{\rho_G\omega^2}{2} \\ &\quad \left. + 2\left[150\frac{\mu(1-\varepsilon)^2\omega_0}{d_P^2\varepsilon^3} + 1.75\frac{\rho_G(1-\varepsilon)\omega_0^2}{d_P\varepsilon^3}\right]\Delta\bar{r}\right\}\end{aligned} \tag{18}$$

In the same column, the pressure drop of the counter-current flow of the gas in the catalyst bed ΔP, is equal to that of the cross current flow $\Delta P'$. Therefore,

$$\Delta P = \Delta P' \tag{19}$$

Combining Eqs. (2), (3), (18) and (19), we obtain a simultaneous equation group, which is the dry pressure drop model.

Approximate calculation shows that the sum of pressure drop from ΔP_F, ΔP_M and ΔP_I is less than 5% of ΔP_S, so ΔP_F, ΔP_M and ΔP_I can be ignored and ΔP_S is equal to ΔP_B. From Eqs. (2), (3′), (15′) and (17), we obtain:

$$u_{B,0} = \frac{\sqrt{2(\Delta\bar{r}/l_b)}ru_G}{l_b[F + (1-F)(r/l_b)\sqrt{2(\Delta\bar{r}/l_b)}]} \tag{20}$$

or

$$u_B = \frac{\sqrt{2(\Delta\bar{r}/l_b)}ru_G}{l_b\varepsilon[F + (1-F)(r/l_b)\sqrt{2(\Delta\bar{r}/l_b)}]} \tag{20′}$$

where u_B is the effective axial gas velocity in catalyst bed.

3.2. Irrigated pressure drop

The main differences between the dry pressure drop and the irrigated pressure drop is the friction loss of the gas within the catalyst bed with or without liquid. Therefore, liquid hold-up among the particles within the catalytic bed has a very important effect on the irrigated pressure drop. When the liquid hold-up increases, porosity is decreased and particle diameter is increased. The void fraction in an irrigated bed ε' can be expressed as:

$$\varepsilon' = \varepsilon - h_L \tag{21}$$

where h_L is the liquid hold-up in the catalyst bed. Since there is liquid in the internal part, especially above the load point, the liquid hold-up in the column measured by experiments is not equal to value of h_L. Therefore, we express the liquid hold-up by an empirical formula, Eq. (22):

$$h_L = au_L^b u_B^c(1-F)^d\left(\frac{H}{n}\right)^e \tag{22}$$

where

$$u_L = \frac{u_{L,0}}{(1-F)\varepsilon} \tag{23}$$

The change in particle diameter can be described by:

$$\frac{1-\varepsilon'}{(d'_P)^3} = \frac{1-\varepsilon}{d_P^3}$$

or

$$d'_P = d_P\left[\frac{1-\varepsilon'}{1-\varepsilon}\right]^{1/3} \tag{24}$$

If Eqs. (20), (21), (22) and (24) are substituted into Eq. (3), the irrigated pressure drop per unit bed height can be calculated.

4. Results and discussion

4.1. Estimating parameters

The calculated results from the mathematical models have been compared with experimental data in Figs. 4 and 6–8. For the irritated pressure drop, the deviation of the calculated values is neglectable at a lower gas–liquid velocity, but it is nonnegligible at a higher gas–liquid velocity when the pressure drop changes very quickly with the increase of gas–liquid velocity. The first reason of the deviation is that a little deviation of the liquid hold-up calculated by Eq. (22) will have an evident effect on the calculated pressure drop when the operation is near the flooding; the other reason may be that the precision accuracy of the experimental data is not high enough; the third reason is that the actual flow

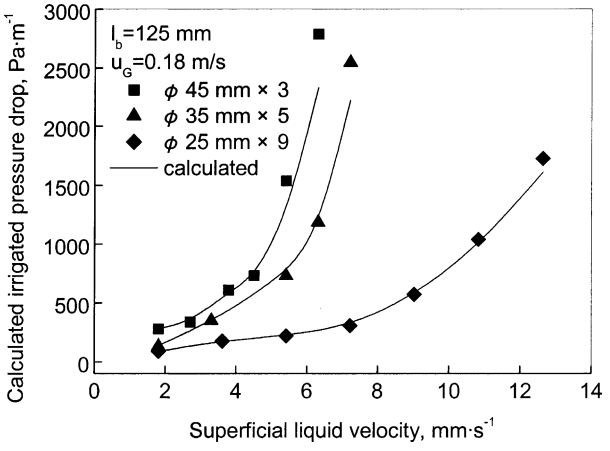

Fig. 4. Relationship between the pressure drop and the superficial liquid velocity for the internals with different outer diameters.

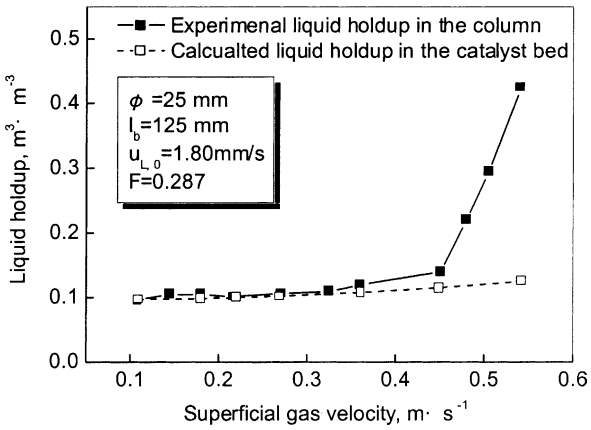

Fig. 5. Comparison between the calculated liquid hold-up in the catalyst bed and experimental liquid hold-up in the column.

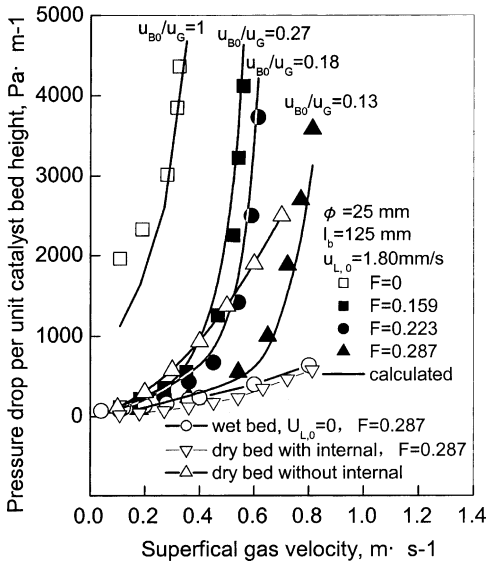

Fig. 6. Relationship between the pressure drop and the superficial gas velocity for the beds loaded with internals of different volume fractions.

behaviors of gas and liquid deviate from that in the ideal flow model.

The parameters in Eq. (22) can be estimated by fitting the experimental data to the mathematical model. We obtain:

$$h_L = 1.18 u_L^{0.32} u_B^{0.25} (1 - F)^{0.158} \left(\frac{H}{n}\right)^{0.158} \quad (25)$$

Fig. 5 shows that the comparison between the liquid hold-up in the catalyst bed calculated by Eq. (25) and that in the column obtained by experiments [7,21]. We can see that both of the calculated and experimental liquid hold-ups are similar when the liquid load is below the load point, but the former is less than the later above the load point. The reason is that capillary effects draw liquid into the catalyst bed below the load point and the excess liquid leaves the catalyst bed and goes into the internal part above the load point.

4.2. The influence of internals on the pressure drop

Fig. 6 illustrates the relationships between the pressure drop per unit catalyst bed height and the superficial gas velocity when internal parts of different volume fractions F are added into the bed. The pressure drop in the catalyst bed with internal parts is much lower than that without internal parts. Moreover, with the increase of the volume fraction of the internal, the pressure drop of the catalyst bed decreases. Obviously, these internal parts can reduce the pressure drop and ameliorate operational flexibility.

Fig. 6 gives the value of $u_{B,0}/u_G$ of the different experiments using different internals. It shows that the superficial gas velocity $u_{B,0}$ for counter-current flow with the internals is much less than that without internal parts. When the volume fractions of the internal parts are 0.159, 0.223 and 0.287, $u_{B,0}$ is 27, 18 and 13% of that without internal parts. This is because the internal parts cause a large amount of gas to flow in the cross current pattern. In addition, from Eq. (25), we can see that the liquid hold-up h_L will decrease with increases of the volume fraction of the internal parts F and the decrease of gas velocity u_B. The decreases of $u_{B,0}$ and h_L cause the decrease in the pressure drop.

4.3. The influence of the diameter of the spiral springs on the pressure drop

To study the effect of the diameter of the springs on the pressure drop, three internal parts whose volume fractions are nearly 30% (Table 1) are manufactured, which are made of nine spiral springs of Φ 25 mm, five spiral springs of Φ 35 mm, and three spiral springs of Φ 45 mm, respectively.

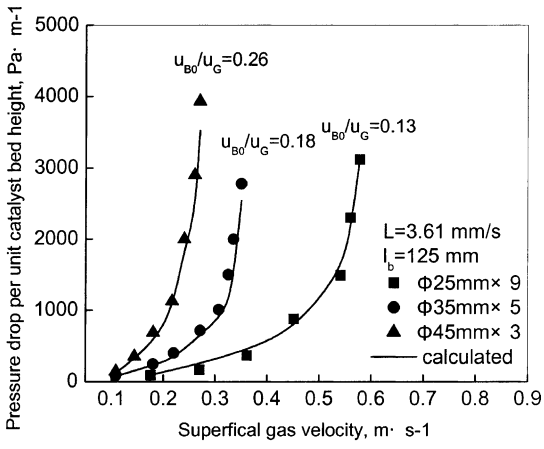

Fig. 7. Relationship between the pressure drop and the superficial gas velocity for the internals with different outer diameters.

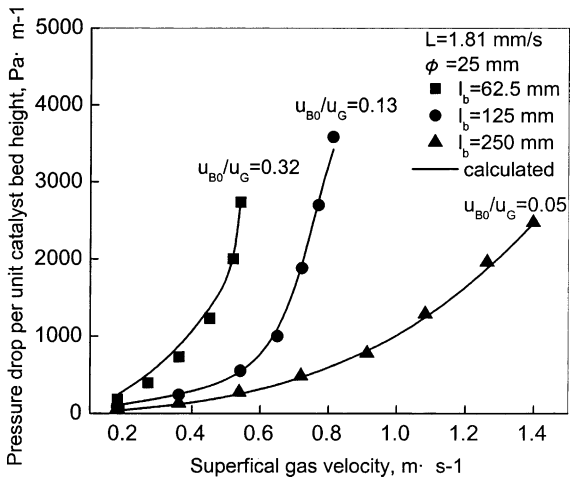

Fig. 8. Relationship between the pressure drop and the superficial gas velocity for the internals with different heights of the stages.

Fig. 7 presents the pressure drop curves for the three internal parts. The operational flexibility deteriorates with increasing outer diameter of the spiral springs when the volume fraction of the internal parts, the liquid flux and the height of the stages are almost the same.

With an increase in the diameter of the spring, $u_{B,0}$ increase, which results in an increase of h_L. The increases of $u_{B,0}$ and h_L cause large pressure drops. So the diameter of the springs should not be too large.

4.4. The influence of the height of the stages on the pressure drop

Fig. 8 shows the influence of the height of the stages on the pressure drop of the catalyst bed. With increasing height of the stages, the operational flexibility improves when the volume fraction of the internal parts, the liquid flux and the diameter of the spiral springs are nearly same.

When the height of the stages decreases, $u_{B,0}$ increases, which results in an increase of h_L. The increases of $u_{B,0}$ and h_L causes large pressure drops. So the height of the stages should not be too small.

On the other hand, it is not good to extend the height of the stages. One of the reasons for installing the baffles is to prevent the gas from escaping through the hollow spiral springs. With respect to the catalytic reactions, more contact of the gas and the liquid with the catalysts leads to more use of the catalysts. Since there is almost no resistance inside the spiral springs, the main gas body flows up vertically in the spiral springs and flows out radially through the wall pores when hitting the baffle. If the height of the stages is too large, some gas does not contact some parts of the catalyst bed and such catalysts are wasted. Therefore, the height of the stages has to be adjusted according to the individual reaction system.

5. Conclusions

On the assumption that the internal part divides the gas flow into two branches, one of which contacts liquid in a conventional counter-current flow and the other in a new cross current flow, a pressure drop model is developed. The irrigated pressure drop calculated by the model in this work does not agree well with experimental data, but the model can be used to explain other experimental results reasonably well.

The model shows that the gas velocity for counter-current flow in the column with internal parts of 15–30% volume fraction is about 30–5% of that without the internal parts and more gas flows in the cross current pattern. The internal part can hold superfluous liquid and reduces the effective liquid hold-up in the catalyst bed. The decreases in the gas velocity and the liquid hold-up make the pressure drop low.

It is expected that the deviation of the model in this work will be considerably reduced in large-scale experiments in which the wall effect is much less, so further research is necessary for the scale-up of the internal part.

References

[1] J.L. DeGarmo, V.N. Parulekar, V. Pinjala, Consider reactive distillation, Chem. Eng. Progr. 3 (1992) 43.
[2] M.F. Doherty, G. Buzad, Reactive distillation by design, Trans. IchemE 70A (1992) 448.
[3] J.G. Stichlmair, T. Frey, Reaction distillation process, Chem. Eng. Technol. 22 (1999) 95.
[4] R. Taylor, R. Krishna, Modelling reactive distillation, Chem. Eng. Sci. 55 (2000) 5183.
[5] G.P. Towler, S.J. Fery, Reactive distillation, in: S. Kulprathipanja (Ed.), Reactive Separation Processes, Taylor & Francis, London, PA, 2000 (Chapter 2).
[6] M. Han, H. Lin, Y. Jin, Catalytic Distillation Apparatus, CA Patent, ZL 99107320.7 (1998) (in Chinese).
[7] M. Han, H. Lin, J. Wang, Y. Jin, Characteristics of the reactive distillation column with a novel internal, Chem. Eng. Sci. 57 (2002) 1551.
[8] H. Lin, M. Han, Z. Wang, J. Wang, Y. Jin, Study on a catalytic distillation column with a novel internal, Chem. Eng. Commun. 189 (2002) 1498.
[9] V. Specchia, G. Baldi, Pressure drop and liquid holdup for two phase concurrent flow in packed beds, Chem. Eng. Sci. 32 (1977) 515.
[10] J.L. Bravo, J.A. Rocha, J.R. Fair, Pressure drop in structured packing, Hydrocarbon Process. 65 (1986) 45.
[11] J.G. Stichlmair, J.L. Bravo, J.R. Fair, General model for prediction of pressure drop and capacity of countercurrent gas/liquid packed columns, Gas. Sep. Purif. 3 (1989) 19.
[12] L. Spiegel, W. Meier, Generalized pressure drop model for structured packings, Institution of Chemical Engineers Symposium Series Distillation and Absorption'92, vol. 2 (128), 1992, pp. B85–B94.
[13] E. Brunazzi, A. Paglianti, Mechanistic pressure drop model for columns containing structured packings, AIChE J. 43 (1997) 317.
[14] H. Subawalla, C. Gonzalez, A.F. Seibert, J.R. Fair, Capacity and efficiency of reactive distillation bale packings: modeling and experimental validation, Ind. Eng. Chem. Res. 36 (1997) 3821.
[15] J. Ellenberger, R. Krishna, Counter-current operation of structured catalytically packed distillation columns: pressure drop, Chem. Eng. Sci. 54 (1999) 1339.

[16] P. Moritz, H. Hasse, Fluid dynamics in reactive distillation packing Katapak-S, Chem. Eng. Sci. 54 (1999) 1367.
[17] L.A. Robbins, Improve pressure-drop prediction with a new correlation, Chem. Eng. Prog. 5 (1991) 87.
[18] M. Han, H. Lin, J. Wang, Y. Jin, Liquid holdup for two phase counter-current flow in the packed column with a novel internal, Ind. Eng. Chem. Res. 41 (2002) 4435.
[19] J.M. Coulson, J.F. Richardson, Flow in pipes and channels, Chemical Engineering, vol. 1, fifth ed., Butterworths, Oxford, 1996 (Chapter 3).
[20] Acrivos, B.D. Babcock, R.L. Pigford, Flow distributions in manifolds, Chem. Eng. Sci. 10 (1959) 112.
[21] E.J. Greskovich, J.T. O'bara, Perforated-pipe distribution, IEC Process Design Dev. 4 (1968) 593.